

行政院國家科學委員會專題研究計畫 期中進度報告

穿越奈米孔洞高分子動態行為之研究(2/3)

計畫類別：個別型計畫

計畫編號：NSC92-2214-E-002-003-

執行期間：92年08月01日至93年07月31日

執行單位：國立臺灣大學化學工程學系暨研究所

計畫主持人： 譚玉真

報告類型：精簡報告

處理方式：本計畫可公開查詢

中 華 民 國 93 年 5 月 17 日

Effect of solvent quality on the conformations of a model comb polymer

鄭光鈴、譚玉真*

臺北市國立臺灣大學化學工程學系

國科會計劃編號：NSC 9-2214-E-002-003

摘要：

The effect of solvent quality on the equilibrium structure of a densely-branched comb polymer is investigated based on the structure factor analyses by off-lattice Monte Carlo simulations. Firstly, theta temperature (θ_∞) must be determined to identify the solvent condition. We locate the characteristic temperature, $\theta_A(N)$, at which the second virial coefficient vanishes and the transition temperature, $\theta_R(N)$, at which radius of gyration, R_g , of the chain varies most rapidly with temperature, i.e. $d^2 R_g / dT^2 \Big|_{\theta_R} = 0$. N represents the total number of monomers of a comb. As $N \rightarrow \infty$, θ_A and θ_R coincide to a point that is identified as the true theta temperature (θ_∞). The structure factors of the main chain, the side chain, and the whole polymer are calculated, respectively. It is found that at $T = \theta_\infty$, the structural factors $S(qR_g)$ for the overall comb polymers match quite well with those of their Gaussian counterparts. When $T < \theta_\infty$, the overall comb polymer assumes collapsed conformations, similar to a homogeneous sphere. However, the structure factor of the side chain indicates that it always remains in an expanded state regardless of the solvent condition. It is attributed to the strong interactions between side chains. The same effect leads to enhanced rigidity of the main chain in comparison to the linear chain, as clearly observed from the rescaled Kratky plot

關鍵字： Monte Carlo simulations, comb polymers, second virial coefficient, structural factor

前言

The polymeric structural units may be connected in all kinds of patterns. Linear-type polymers are the simplest of all. Nonlinear type polymers, including star, knotted or branched structures, are also frequently encountered in the polymeric applications. A regularly branched polymer (also called a comb polymer) with side chains of equal length has rather interesting topology. Its geometric conformations as well as thermodynamic properties are quite different from those of a linear chain due to steric repulsion between high-density monomers. These interactions result in the swelling of the comb on a large scale.¹ Grafting of side chains onto the main chain also greatly affects the equilibrium structure of the main chain of the comb molecule. Partial stretching of the backbone was observed.¹⁻¹² The degree of induced rigidity of the backbone varies with several factors, such as side-chain length, side-bead size and distance between grafted point. However, solvent quality may also play an important role in the conformations of the combs. The systems studied in most of the previous works were in good solvent (or athermal) conditions. In his work, Rouault³ introduced attractive interactions between side-chain monomers. At high temperature, the ratio between the radius of gyration of the main-chain of the comb polymer and that of a linear chain without side chains is about 2 ($R_g^2 main / R_g^2 linear \approx 1.9$), indicating a swollen conformation as a result of the repulsion between side chains. On the other hand, at low temperature, $R_g^2 main / R_g^2 linear \approx 1$, showing that the side chains are shrunk below their excluded volume radius to a radius very near the Gaussian value. The comb polymer could be seen as an excluded volume chain decorated with Gaussian side-chains. For a more realistic chain with attractive interactions among all the monomers on the comb, the effect of solvent quality (or system temperature) on the conformations of the main chain, side chains and overall comb polymer is still unclear.

The theta point (θ) of macromolecules is traditionally viewed as the point at which intrachain excluded volume interactions exactly cancel the attractive interactions between monomers of the chain,¹³ Consequently, at θ temperature, monomers on a polymer molecule telescope one another freely without any net interaction. In other words, they behave quasi-ideally, i.e., $\langle R_g^2 \rangle^{1/2} \sim N^{1/2}$ for linear chains. N is the total number of monomers. θ temperature is also defined for a polymer solution as the Boyle point of a real gas as the polymer-polymer

second virial coefficient vanishes. Furthermore, according to Flory's theory,¹³ the theta temperature may be identified as the critical miscibility temperature in the limit of infinite molecular weight. Simulation results suggested that a consistent θ temperature was found for these three definitions, however, in the limit of infinite chain length.¹⁴ Study of the theta point of knotted polymer chains again supported the findings.¹⁵

For comb polymers, θ point is expected to shift from its linear counterpart'. Gallacher and Windmer¹⁶ thought that the high nearest neighbor density expected in the branched polymers would lead to a θ point at a much higher temperature. On the other hand, Rouault³ believed the value of temperature needed to reach the θ point for grafted chains in the brush is lower than that of linear chains in the bulk. It is important to clarify these differences and then the solvent condition can be identified.

Structure factor which can be measured by neutron or X-ray scattering experiments as well as computer simulations, thus offers a direct connection between simulation and experimental works. Once we have determined the true theta temperature for comb polymers, Monte Carlo simulations can be used to calculate $S(qR_g)$ or $(qR_g)^2 S(qR_g)$ as a function of qR_g to investigate the variation of chain conformation in different solvent quality. As we know, $S(qR_g)$ describes the Fourier components of density fluctuation. It is related, through a three-dimensional Fourier transform to the pair distribution function $g(r)$. Thus, systems with same $S(qR_g)$ may consist of equivalent internal structure. On the other hand, the structure factor plotted as $(qR_g)^2 S(qR_g)$ vs. qR_g is called the rescaled Kratky plot, which has the advantage of being less sensitive on N .¹⁷ In this type of plot, the curve for linear chain situating in good solvents always ascends. However, for rings or other chains with more compact structures, a clear difference is observed. Even under good solvent condition, there are maxima existing within the curves. The sharpness of the peak can be an indication of the compactness of the chain.

In this work, we intend to estimate the θ_∞ temperature of the comb polymers through two different schemes. Firstly, we use the algorithm proposed by Harismiadis and Szleifer⁹ to calculate the second virial coefficient of the comb polymer. Note that similar procedures have been successfully used in various studies.^{15,18-24} Once A_2 is obtained, temperature (A) at which $A_2=0$ can be determined. Secondly, we calculate R_g of the chains and determine the transition temperature (R) at which EMBED Equation.3 . The true theta temperature (θ_∞) is obtained through extrapolating A and R to the infinite chain length regime. Then the structure factors of the comb polymer at temperatures greater than, equal to and less than θ_∞ are calculated to examine the effect of solvent quality on the equilibrium conformations of comb polymers.

研究方法

The model comb polymer studied in this work is modeled as beads connected by springs. Our comb model is quite densely grafted. Figure 1 displays the schematic diagram of a model 10-11 comb polymer, with b , m and s representing the number of beads on a side chain, the number of side chains attached to the main of the comb and the chain length of the spacer separating side chains, respectively. In this work, we consider only the case $s=2$. The interactions between all the nonbonded beads are through the standard Square-Well potentials.

$$U_{nb} = \begin{cases} \infty & (\sigma > r) \\ -\varepsilon & (\lambda\sigma > r \geq \sigma) \\ 0 & (r \geq \lambda\sigma) \end{cases} \quad (1)$$

where ε and σ are the energy and size parameters, respectively and $\lambda=1.5$. The monomeric ε and σ are units used for the reduced quantities for temperature and distances as $T^*=kT/\varepsilon$ and $R^*=R/\sigma$. The interactions between bonded beads are represented by an infinite deep Square-Well potential as

$$U_b = \begin{cases} \infty & (\sigma > r) \\ 0 & (\zeta\sigma > r \geq \sigma) \\ \infty & (r \geq \zeta\sigma) \end{cases} \quad (2)$$

where $\zeta=1.2$.

The systems studied contain a single model comb with total number of monomers, N ranging approximately from 20 to 300. The model polymers are labeled as b - m . We have studied the model comb polymers up to 33 different configurations with $b=5,10,15$ and $m=1,2,3,4,6,7,9,10,12,13,15$. The simulations are performed under the conditions of constant temperature and total number of beads.

For convenience, the initial configurations of chains studied are constructed on a lattice. The construction process is quite straightforward but the topological constraint must be conserved. Once the initial configurations are created, the simulations are carried out in continuous space. The trial moves employed for chains of the equilibration and production process are bead displacement motions which involve randomly picking a bead and

displacing it to a new position in the vicinity of the old position. The distance away from the original position is chosen with probability that the condition of equal sampling of all points in the spherical shell surrounding the initial position must be satisfied. The new configurations resulting from this move are accepted according to the standard Metropolis acceptance criterion.²⁵ The samples for the statistical averages are taken every N MC steps and the total number of MC steps is over $(10^7)N$.

(a) Radius of gyration

The root-mean-squared radius of gyration of the polymer chains was determined by

$$\langle R_g^2 \rangle^{1/2} = \left\langle \frac{\sum_{i=1}^N [(x_i - x_{CM})^2 + (y_i - y_{CM})^2 + (z_i - z_{CM})^2]}{N} \right\rangle^{1/2} \quad (3)$$

where (x_i, y_i, z_i) are the coordinates of the i th monomer on the chain and (x_{CM}, y_{CM}, z_{CM}) are the coordinates of the center of mass of the comb. The angular bracket $\langle \dots \rangle$ denotes ensemble average.

(b) Second virial coefficient

The virial expansion for the compressibility factor takes the form²⁶

$$\beta P / \rho = 1 + A_2 \rho + A_3 \rho^2 + \dots \quad (4)$$

where P is the pressure, ρ is the molecular number density of the system. A_2, A_3 are the second and third virial coefficients, respectively. $\beta = 1/kT$ where k is the Boltzmann's constant and T is the temperature.

To calculate the second virial coefficient, we used the algorithm proposed by Harismiadis and Szleifer.¹⁸ The second virial coefficient can be calculated in terms of the interaction potentials from standard statistical mechanics^{19,20}

$$A_2 = 2\pi \int \left(1 - \exp \left[- \frac{F_2(\xi) - 2F_1}{kT} \right] \right) \xi^2 d\xi \quad (5)$$

where F_1 is the Helmholtz free energy of a single chain at infinite dilution in a solvent, and $F_2(\xi)$ is the Helmholtz free energy of a system composed of the same solvent and two polymer molecules when their center of mass distance is ξ . The difference in the exponential can be thought of as an effective potential between the chain molecules, i.e.

$$U_{eff}(\xi) = F_2(\xi) - 2F_1 = -kT \ln \langle \exp[-\beta U_{inter}(\xi)] \rangle \quad (6)$$

where U_{inter} is the intermolecular interaction energy between the two polymer molecules. However, note that each chain does not know the presence of the other chain. $\langle \dots \rangle$ denotes a canonical average over all the configurations of the two chains. If there are no overlaps, it equals to the number of segment pairs belonging to the two interacting polymers with distance lying between σ and 1.5σ , multiplied by the well depth. A trial move leading to overlap of two molecules is allowed but yields an infinite value of intermolecular interaction, i.e. $U_{inter} = \infty$. To calculate U_{inter} , for a given separation (ξ) between two comb polymers, two steps are involved in obtaining samples in the phase space. First, a lot of different conformations for the polymers are generated. Secondly, for given conformations of the two polymers, different relative orientations yield different interaction energies. As a result, the "rotation" is simply an efficient way to obtain more interaction energy samples. Of course, one can always adopt the first step only, but the approach is much less efficient. As mentioned, the algorithm used to calculate U_{eff} and then A_2 has already been used in various studies.¹⁸⁻²⁴ Our previous study¹⁵ of A_2 of a knotted chain has more detailed descriptions of the procedure.

(c) Static structure factor

The structure factor describes the Fourier components of density fluctuations in the system. It can be measured by neutron or X-ray scattering experiments as well as computer simulations. The structure factor of a single chain is defined as^{25,27}

$$S(q) = \frac{1}{n^2} \sum_{i=1}^n \sum_{j=1}^n \exp \langle -iq \cdot r_{ij} \rangle \quad (7)$$

where n is the number of scattering units; r_{ij} is the vector joining two scattering points i and j of the same molecule. The bracket $\langle \dots \rangle$ means that $S(q)$ is taken over all conformations and orientations. For a randomly oriented chain, eq.(7) can be expressed as

$$S(q) = \frac{1}{n^2} \sum_{i=1}^n \sum_{j=1}^n \left\langle \frac{\sin qr_{ij}}{qr_{ij}} \right\rangle \quad (8)$$

結果與討論

Monte Carlo simulations were performed to study the effect of solvent quality (temperature) on the equilibrium conformation of comb-like polymers with different architectures. To do so, we start the work by determining the true theta temperature (θ_∞) of the system. First, the theta temperature (θ_A) at which the second virial coefficients for chains of finite length vanish is calculated. Figure 2 shows the calculated second virial coefficients A_2 for comb-like polymers of which $b=15$ and $m=1,2,3,4$, respectively, as a function of temperature. The qualitative behavior of the virial coefficient of the comb-like polymer is the same with its linear counterpart. At low temperatures, the attractive interactions dominate and A_2 is negative. A_2 increases as the temperature increases. There exists a temperature (that is, the theta temperature, θ_A) where the attractive and the repulsive intermolecular interactions exactly cancel each other and thus $A_2=0$. Below theta temperature, the longer the chain length, the more negative the second virial coefficient is. On the other hand, above theta temperature, A_2 for longer chain becomes more positive than that of the shorter chain. Note that the true *theta* temperature (θ_∞) is in fact the temperature at which the second virial coefficient of infinitely long chains is zero. However, θ_A is known to be a fairly weak function of N .^{14,20,28,29} Thus we intend to estimate θ_∞ by extrapolating θ_A to infinite chain length. It is also worth mentioning that combs 15-1 and 15-2 are very similar to linear chains of 17 and 32 monomers carrying one or two very short chains of two monomers each. Moreover, combs carrying side chains of about the same length as (or longer than) the main chain may show some crossover to star-like polymers.⁴

For a comb polymer with the same number of monomers on a side chain (i.e. $b=\text{constant}$), θ_A decreases slightly as number of side chain, m , increases. On the other hand, when m is fixed, θ_A also decreases with increasing number of monomers on each side chain, b . Generally speaking, θ_A of a comb polymer decreases as the total number of monomers N increases. It is known that polymers with the same molecular mass can exhibit different physical behaviors due to different topological architectures. For example, molecules with more complex structures often have smaller radii of gyration.³⁰ In the experimental work of Roovers et al.,^{31,32} theta point depressions were observed for ring-type polymer chain when compared to a linear polymer chain of the same molecular weight. The degree of depression is only about 3%. In this work we observed a similar degree of depression in the θ_A for the comb-like chains. The *theta* temperature of infinite molecular weight, i.e. θ_∞ , can be estimated to be about 2.53. We will have more discussion on this later in this section.

As we know, *theta* point can also be the temperature at which the intrachain excluded volume interactions exactly cancel the intrachain attractive interactions. For linear chains, at *theta* temperature $\langle R_g^2 \rangle^{1/2} \sim N^{\nu} \nu \approx 1/2$, whereas in a good solvent $\nu \approx 3/5$. For comb-like polymers, the mean-squared radius of gyration of the entire molecule was found to increase monotonously with increasing N .^{4,12,33} However, the simple relation of $\langle R_g^2 \rangle^{1/2} \sim N^{1/2}$ does not hold for the comb-like chains and a valid expression for combs with varying b and m is not available at the moment. It is worthy of mentioning that Rouault and Borisov¹ have studied the global conformations and the radius of gyration of comb-branched polymers by using both Monte Carlo simulations and scaling analysis. However, the scaling theory is analyzed only as functions of the length of the side chains and spacers. The effect of number of side chain was not considered.

Radius of gyration of the entire comb-like chain as a function of temperature is shown in Figure 3. At low temperatures, the intrachain attractive interaction dominates and the chain assumes compact structure. At high temperatures, the chain takes on an expanded conformation. Again, at *theta* temperature, the intrachain attractive interactions will compensate exactly the influence of volume exclusion. When this condition is achieved, the polymer chain will assume its so-called random flight configuration. For a linear chain, at theta condition, $\langle R_g^2 \rangle^{1/2}$ is proportional to $N^{1/2}$. Therefore at theta temperature, the curves $\langle R_g^2 \rangle^{1/2}/N^{1/2}$ belonging to all chain lengths N will intersect at a single point. However, as mentioned, $\langle R_g^2 \rangle^{1/2} \sim N^{1/2}$ does not hold for the comb-like chains. The intersection scheme can not be applied to locate the theta point of the system. Therefore another method has been employed in this work. We have numerically differentiated the R_g curve with respect to T and defined the maximum point of the resulting curve as the transition temperature (θ_R). Note that the transition temperature does not necessarily coincide with θ_A for chain of finite length. In fact, in the study of linear chains, θ_R is found to be lower than θ_A . However, we expect that the θ_R and θ_A will become the same in the limit of infinite chain length.

We have plotted in Figure 4, all the θ_A and θ_R as a function of $1/N$. It is fairly obvious that for chains with larger m , θ_R continues to rise. The extrapolation of θ_R to chains of infinite chain length is believed to converge to the same temperature regime for all the comb-like polymers studied. Also in the infinite chain length regime, $N \rightarrow \infty$, theta temperatures determined through two different definitions - the vanishing of the second virial coefficient $A_2=0$, and the quasi-ideal behavior of the radius of gyration are expected to coincide into a single value which is the true theta temperature ($\theta_\infty \approx 2.53$).

Now that we have determined the true theta temperature (θ_∞) for comb polymers, Monte Carlo simulations can be used to calculate $S(qR_g)$ as a function of qR_g to investigate the variation of chain conformation in different solvent conditions (i.e. at different system temperatures). We have performed the calculations of $S(qR_g)$ for several different types of comb polymers at θ_∞ estimated in this work. The $S(qR_g)$ of the corresponding Gaussian combs are also calculated. $S(qR_g)$ calculated for the overall comb polymers are found to match quite well with those of their Gaussian counterparts as shown in Figure 5. As we have mentioned before, $S(qR_g)$ describes the Fourier components of density fluctuation. It is related, through a three-dimensional Fourier transform to the pair distribution function $g(r)$. Thus, systems with the same $S(qR_g)$ may consist of equivalent internal structure. Although the radius of gyration of the Gaussian comb polymer is smaller than that of the model polymer, Figure 5 reveals that the structure factors can be the same if the wave vector q is scaled by R_g and indirectly verifies the accuracy of the θ_∞ temperature estimated in this work.

Comb polymers have more compact structures than linear chains do. Thus, we expect to see the $(qR_g)^2 S(qR_g)$ vs. qR_g curves going through maxima at certain qR_g even when system is at good solvent condition (i.e. $T > \theta_\infty$). We have shown in Figure 6, the Kratky plot of 5-10 comb polymer at three different solvent conditions. All three curves go through maximum as anticipated. However, as we have mentioned before, the sharpness of the peak can be an indication of the compactness of the chain. Thus, as temperature increases, the curves gradually flatten revealing that the comb is becoming more expanded. Note that in Figure 6, we have also plotted the structure factor for a homogeneous sphere^{27,34} of a radius R , $(qR_g)^2 S(qR_g) = (qR_g)^2 [3(\sin qR - qR \cos qR)/(qR)^3]^2$, where $R_g = (3/5)^{1/2} R$. As we can see, at $T=1.2$, i.e. below the θ_∞ regime, the solvent is poor and the polymer takes on a collapsed conformation fairly similar to a spherical structure. On the other hand, above the θ_∞ regime, the chain is in a comparatively more expanded state. It is also worth mentioning that for small qR_g we have the same identical behavior, $(qR_g)^2 S(qR_g) = (qR_g)^2 (1 - (qR_g)^2/3 + \dots)$ as shown in Figure 6.

The Kratky plot of the main chain of 10-10 comb at $T=10$, θ_∞ and 1.2 are shown in Figure 7. The $(qR_g)^2 S(qR_g)$ curves of the corresponding linear chain without side chains are also plotted. At $T=10$, the $(qR_g)^2 S(qR_g)$ curve of the main chain ascends much faster than that of a normal linear chain. At $T=1.2$, the $(qR_g)^2 S(qR_g)$ curve of the main chain is more level than that of the normal linear chain. These results clearly indicate that the interactions between side chains induce rigidity upon the main chain. That is, the conformation of the main chain is more expanded than the conformation of a normal linear chain at the same temperature. Also, as we can see from Figure 7, the $(qR_g)^2 S(qR_g)$ curve of the main chain at $T=10$ is situated in between those of a rod and a linear chain. Therefore, R_g of the main chain now scales with N^ν with $0.588 < \nu < 1$. The actual ν value can be obtained by plotting $S(qR_g)$ of the main chain as a function of qR_g in a log-log plot. Theory predicts that at large qR_g ($qR_g > 1$) one should have $S(qR_g)$ proportional to $(qR_g)^{-1/\nu}$, ν being the Flory exponent.^{4,12} Here, we found that at $T=10$, $\nu=0.69$. This result is consistent with the work of ref 4. However, the fact that the $(qR_g)^2 S(qR_g)$ curve of the main chain at $T=1.2$ goes through a maximum indicates that the structure of main chain collapses at temperature below θ_∞ in spite of the inflexibility caused by the side chain excluded volume effect. Nonetheless, the conformation of the main chain at $T=1.2$ still is more expanded than a homogeneous sphere structure. Note that the induced rigidity on main chain occurs only when the spacer length between the side chains is short compared to the side-chain length, i.e., for densely branched, comb polymers. If spacer length is much longer than the side-chain length, the main chain will behave very much like a normal linear chain.

Figure 8 shows the $(qR_g)^2 S(qR_g)$ curves of the side chains of 10-10 comb. It is not surprising to see that the $(qR_g)^2 S(qR_g)$ curve ascends with increasing qR_g when $T=10 > \theta_\infty$, and the curve coincides well with that of a normal linear chain in good solvents. For temperature below θ_∞ , normal linear chains already exhibit collapsed configurations. However, as can be seen from Figure 8, for all the temperatures studied, $(qR_g)^2 S(qR_g)$ curves of the side chains of 10-10 comb keeps ascending with increasing qR_g indicating that these side chains always stay in expanded state regardless of the solvent conditions. Our results are consistent with the theoretical work of Shiokawa et al²⁴ for polymacromonomers with long side chains. In their work, they observed that the shape of the main chain is gradually varied with increasing b , from a self-avoiding coil-like structure to an extended rod-like form. Nevertheless, the side chains maintain a three-dimensional self-avoiding coil-like form irrespective of the conformation of the main chain. Evidently, their approaches correspond to the densely branched conformations of the comb polymer. For temperature below θ_∞ , the whole comb is actually in collapsed state and side chains are closely intertwined with each other. However, from the point of view of a single side chain, the conformation is always in extended state because of the excluded volume effect associated with the interacting side chains.

In this paper we have studied the effect of solvent quality on the equilibrium structure of a densely-branched comb polymer through the analyses of structure factors calculated. The true theta temperature θ_∞ for comb polymers is firstly determined to classify the solvent quality. We found that when $T=\theta_\infty$, the

structure factor of a comb polymer agrees quite well with that of its Gaussian counterpart. The comb polymer expands as $T > \theta_{\infty}$ and collapses into a globule-like structure as $T \ll \theta_{\infty}$. Main chains of the combs behave as whole combs do, except that enhanced rigidity is clearly observed from the rescaled Kratky plot for all kinds of solvent conditions. Strong interactions between side-chains are the key factor of the conformations resulted. The Kratky plot of the side chain indicates that it stays in an expanded state at all times irrespective of the solvent conditions as a result of the very same effect.

參考文獻

1. Y. Rouault and O.V. Borisov, *Macromolecules*, 29, 2605 (1996).
2. M. Saariaho, I. Szleifer, O. Ikkala, and G. Brinke, *Macromol. Theory Simul.* 7, 211 (1998).
3. Y. Rouault, *Macromol. Theory Simul.* 7, 359 (1998).
4. S. Elli, F. Ganazzoli, E. G. Timoshenko, Y. A. Kuznetsov and R. Connolly, *J. Chem. Phys.* 120, 6527 (2004).
5. M. Saariaho, O. Ikkala, I. Szleifer, I. Erukhimovich and G. Brinke, *J. Chem. Phys.* 107, 3267 (1997).
6. E. G. Timoshenko, Y. A. Kuznetsov and R. Connolly, *J. Chem. Phys.*, 116, 3905 (2002).
7. M. Saariaho, A. Subbotin, I. Szleifer, O. Ikkala, and G. Brinke, *Macromolecules*, 32, 4439 (1999).
8. R. Djalali, S.-Y. Li, and M. Schmidt, *Macromolecules*, 35, 4282 (2002).
9. S. Lecommandous, F. Checot, R. Borsali, M. Schappacher, A. Deffieux, A. Brulet and J. P. Cotton, *Macromolecules*, 35, 8878 (2002).
10. M. Saariaho, A. Subbotin, O. Ikkala and G. Brinke, *Macromol. Rapid Commun.* 21, 110 (2000).
11. K. Fischer and M. Schmidt, *Macromol. Rapid Commun.* 22, 787 (2001).
12. P. G. Khalatur, D. G. Shirvanyanz, N. Y. Starovoitova, and A. R. Khokhlov, *Macromol. Theory Simul.* 9, 141 (2000).
13. P.J. Flory, Cornell University Press: Ithaca, NY (1953).
14. Y.-J. Sheng, A. Z. Panagiotopoulos, S. K. Kumar and I. Szleifer, *Macromolecules* 27, 400 (1994).
15. Y.-J. Sheng and C.-S. Liao, *J. Chem. Phys.* 118, 4748 (2003).
16. S. J. Gallacher and S. J. Windmer, *J. Chem. Phys.* 44, 1139 (1966).
17. E.G. Timoshenko, Y. A. Kuznetsov, and R. Connolly, *J. Chem. Phys.* 116, 3905 (2002).
18. V. I. Harismiadis and I. Szleifer, *Molecular Physics* 81, 851 (1994).
19. C. G. Gray and K. E. Gubbins, *Theory of Molecular Fluids*; Clarendon Press: Oxford, UK, 1982.
20. V. I. Harismiadis and I. Szleifer, *Molecular Physics* 81, 851 (1994).
21. D. A. McQuarrie, *Statistical Thermodynamics* (New York: Harper & Row), 1976.
22. H. Yamakawa, *Modern Theory of Polymer Solutions*; Harper and Row: New York, 1971.
23. J. Dautenhahn and C. K. Hall, *Macromolecules* 27, 5399 (1994).
24. A. Yethiraj, K. G. Honnell and C. K. Hall, *Macromolecules* 25, 3979 (1992).
25. M. P. Allen and D. J. Tildesley, *Computer Simulations of Liquids*, Oxford University Press: New York (1987).
26. C. G. Gray and K. E. Gubbins, *Theory of Molecular Fluids*; Clarendon Press: Oxford, UK, 1982.
27. C. Oh and C. M. Sorensen, *Phys. Rev. E*, 57, 784 (1998).
28. W. Bruns, *Macromolecules* 17, 2826 (1984).
29. M. Janssens and A. Bellemans, *Macromolecules* 9, 303 (1976).
30. T. Pakula, *Macromol. Symp.* 174, 393 (2001).
31. J. Roovers and P. M. Toporowski, *Macromolecules* 16, 843 (1983).
32. J. Roovers, *J. Polym. Science, Polym. Phys. Ed.* 23, 1117 (1985).
33. K. Shiokawa, K. Itoh and N. Nemoto, *J. Chem. Phys.* 111, 8165 (1999).
34. K. Schmitz, *Dynamic Light Scattering by Macromolecules* (Academic, Boston, 1990).

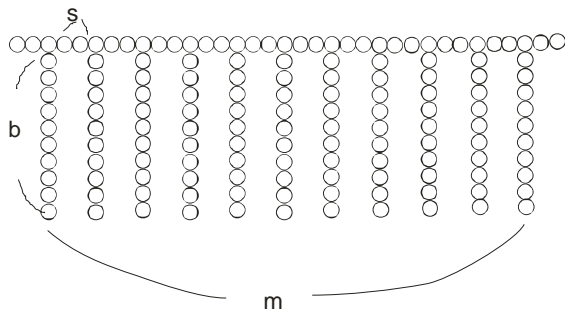


Figure 1. Schematic diagram of a model b - m comb-like polymer. In this case, $b=10$ and $m=11$ representing that the comb has 11 side chains and each side chain has 10 monomers. In this work, s is set to 2 for all the combs studied.

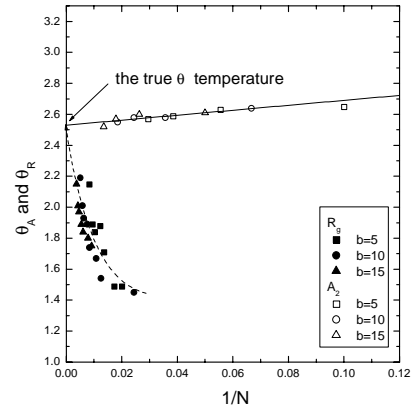


Figure 4. Transition temperature θ_R and θ_A plotted against $1/N$.

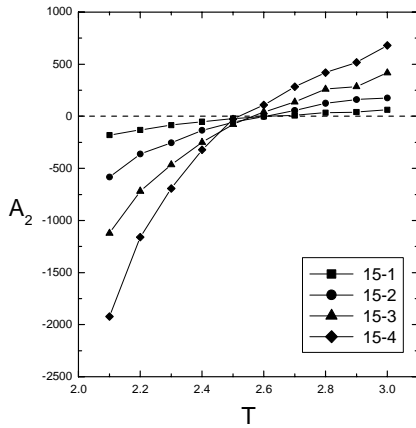


Figure 2. Calculated second virial coefficients A_2 for comb-like polymers as a function of temperature.

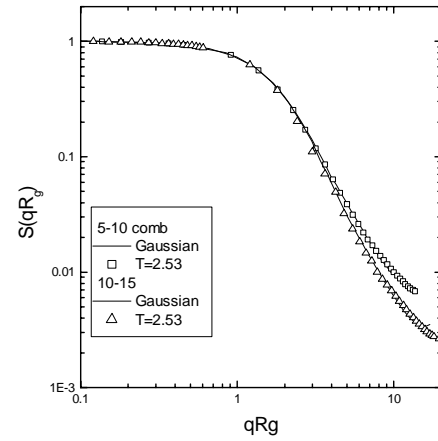


Figure 5. $S(qR_g)$ plotted as a function of qR_g for 5-10 and 10-15 combs.

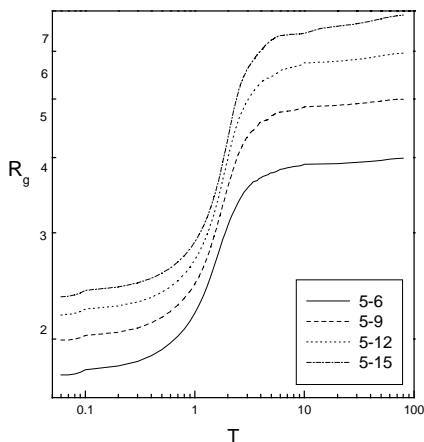


Figure 3. Radius of gyration of the entire comb-like chain as a function of temperature.

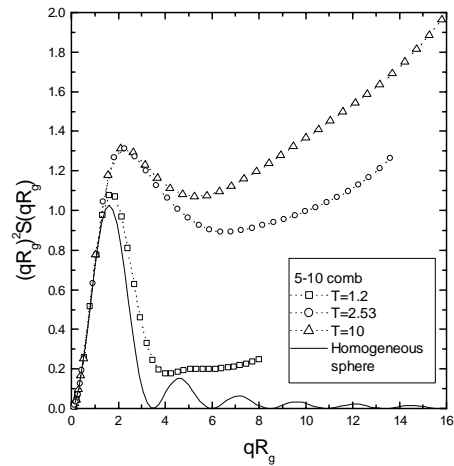


Figure 6. The Kratky plot of 5-10 comb at different temperatures.

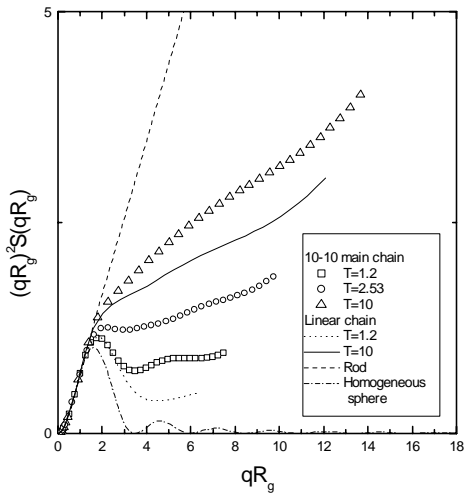


Figure 7. The Kratky plot of the main-chain of 10-10 comb and of the linear chain with $N=32$ at different temperatures.

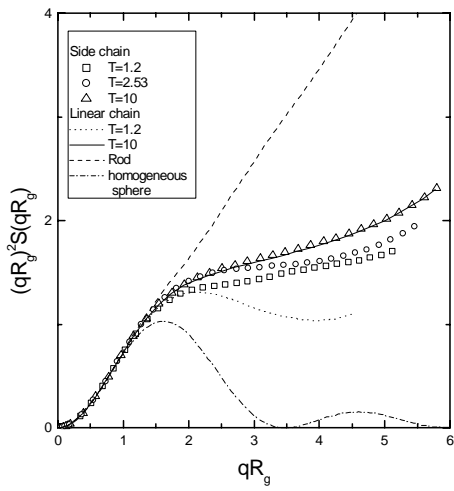


Figure 8. The Kratky plot of the side-chain of 10-10 comb and of the linear chain with $N=10$ at different temperatures.